JOURNAL OF COMPUTATIONAL PHYSICS 14, 93–103 (1974)

Local Errors of Difference Approximations to Hyperbolic Equations*

STEVEN A. ORSZAG†

Flow Research, Inc., Kent, Washington 98031

AND

LANCE W. JAYNE

Department of Mathematics, M.I.T., Cambridge, Massachusetts 02139

Received July 16, 1973

It is shown that the rate of convergence of numerical approximations to the solution of hyperbolic partial differential equations is degraded when the solution being sought is not sufficiently smooth. A pth-order finite-difference scheme may give worse than pth-order convergence if the $(p+1)$st derivatives of the solution are not piecewise continuous. Spectral methods, which are normally expected to give infinite-order convergence, give only finite-order convergence if some derivative of the solution is not continuous. Near a discontinuity propagating along a characteristic of the differential equation, the truncation error of difference approximations is much larger on one side than on the other, and it oscillates in sign on the side where it is larger. (It may also oscillate on the other side of the discontinuity, depending on the order of the numerical scheme used.) Finally our analysis shows that, even if the true solution is not smooth, high-order schemes are more accurate than lower-order schemes.

The formal truncation error analysis of difference schemes for partial differential equations can be misleading if the solution being approximated is not smooth. For smooth solutions, second-order schemes give errors of order h^2 (where h is the grid interval), fourth-order schemes give errors of order h^4, etc. However, convergence rates are degraded when the solution is not smooth. There have been many studies of the effect of loss of smoothness on numerical truncation errors [1–3], but most studies have been couched in terms of error norms and have not elucidated the local structure of the errors induced by local nonsmoothness. In this paper, we study the local structure of errors in the solution of first-order

* This work is supported by Fluid Dynamics Branch, Office of Naval Research, Dept. of Navy, Contract No. N0014-72-C-0355.

† Permanent address: Department of Mathematics, M.I.T., Cambridge, Mass.

hyperbolic partial differential equation. Some of the results obtained below are contained in Refs. [1–3]; it is hoped that the present analysis will make more transparent the general results of Hedstrom and Thomée as well as provide detailed information on the structure of local errors.

A prototype of a mixed initial-boundary value problem for a hyperbolic equation is the wave equation

$$\partial u/\partial t + \partial u/\partial x = 0 \qquad (0 < x < 1, t > 0) \tag{1a}$$

$$u(x, 0) = 0 \qquad (0 < x < 1), \qquad u(0, t) = f(t)(t > 0) \tag{1b}$$

The exact solution is

$$u(x, t) = \begin{cases} 0, & t \leqslant x; \\ f(t - x), & t > x. \end{cases} \tag{2}$$

If $f \in C^\infty[0, \infty]$, then u is C^∞ except possibly on the characteristic $x = t$; $u(x, t)$ has discontinuous nth order derivatives on $x = t$ $(0 < t < 1)$ if $f^{(q)}(0) = 0$ for $q < n$ and $f^{(n)}(0) \neq 0$.

If a pth order numerical scheme is used to solve (1), the maximum error is $0(h^p)$ if derivatives of $u(x, t)$ of order $p + 1$ are piecewise continuous. If this is not the case, it is still true (see below) that the error at a fixed point $x > t$ 'ahead' of the singular characteristic is $0(h^p)$ as $h \to 0$, provided that the exact solution is smooth off $x = t$ (as follows from $f \in C^\infty$) and boundary conditions are imposed carefully (cf. [4, 5]). Errors in the neighborhood of $x = t$ and 'behind' the singular characteristic $(x < t)$ are not $0(h^p)$ but are much larger. The latter errors depend only on the local discontinuity and do not depend on details of boundary and initial conditions [provided the numerical scheme is chosen to be stable and to have boundary-induced errors no larger than $0(h^p)$]. Hence, we make the ansatz that it is possible to analyze the local errors by replacing the actual boundary and initial conditions (1b) by simpler conditions that reproduce the proper discontinuity on $x = t$. A suitable choice for the following analysis is periodic boundary conditions on $0 \leqslant x \leqslant 1$. A solution to (1a) with continuous derivatives of order $q < n$ and a discontinuous nth order derivative $\partial^n u/\partial x^n \,|_{x=t+} - \partial^n u/\partial x^n \,|_{x=t-} = D$ is

$$u(x, t) = D \sum_{\substack{k=-\infty \\ k \neq 0}}^{\infty} \frac{1}{(2\pi i k)^{n+1}} \exp[2\pi i k(x - t)] \tag{3}$$

where k is integral.

With second-order centered differences in space, a semidiscrete approximation to (1a) is

$$\frac{\partial u_2(x, t)}{\partial t} + \frac{u_2(x + h, t) - u_2(x - h, t)}{2h} = 0. \tag{4}$$

Strictly speaking, the difference-differential equation (4) is applied only at the grid points $x = mh$, $1 \leqslant m \leqslant N$, where $N = 1/h$ is the number of grid points; however, the continuous form of (4) is analytically more convenient. As argued above, local errors may be studied by imposing periodic boundary conditions and initial conditions that match the desired discontinuity structure. It follows that the second-order scheme gives the following approximation to (3):

$$u_2(x, t) = D \sum_{\substack{k=-\infty \\ k\neq 0}}^{\infty} \frac{1}{(2\pi ik)^{n+1}} \exp[2\pi ik(x - t \sin 2\pi kh/2\pi kh)].$$

Hence, the local error is given by

$$e_2(x, t) = u(x, t) - u_2(x, t) = -D \sum_{\substack{k=-\infty \\ k\neq 0}}^{\infty} \frac{1}{(2\pi ik)^{n+1}} \exp[2\pi ik(x - t)]$$
$$\times \{\exp[2\pi ikt(1 - \sin 2\pi kh/2\pi kh)] - 1\}. \tag{5}$$

The sum in (5) may be estimated as $h \to 0$ by breaking it into contributions $e_2^{(1)}$ from $0 \leqslant |k| \leqslant 1/h^\alpha$ and $e_2^{(2)}$ from $|k| > 1/h^\alpha$ where $0 < \alpha < 1$. The contribution $e_2^{(2)}$ is clearly $0(h^{\alpha n})$ for all x, t as $h \to 0$, so that by taking α close enough to 1 the contribution of $e_2^{(2)}$ is asymptotically negligible compared to that of $e_2^{(1)}$ for $n \leqslant 2$, as we shall now see. The contribution $e_2^{(1)}$ is estimated by

$$e_2^{(1)} = -D \sum_{|k|\leqslant h^{-\alpha}} \frac{1}{(2\pi ik)^{n+1}} \exp[2\pi ik(x - t)]\{\exp[it(2\pi k)^3 h^2/6] - 1\}[1 + 0(h^{2/3})]$$

since $kh \ll 1$ for all k retained in the sum. If we choose $2/3 < \alpha < 1$, then the resulting sum is a Riemann sum for the integral

$$E_2(\lambda, t) = C \int_{-\infty}^{\infty} \xi^{-n-1} e^{i\lambda\xi}(e^{i\xi^3} - 1)\, d\xi \tag{6a}$$

where $\xi = 2\pi k(h^2 t/6)^{1/3}$,

$$C = \frac{D}{2\pi} i^{-n+1}(h^2 t/6)^{n/3}, \tag{6b}$$

$$\lambda = (6/h^2 t)^{1/3}(x - t). \tag{6c}$$

The final result is that

$$e_2(x, t) \sim E_2(\lambda, t) \qquad (h \to 0) \tag{6d}$$

for all x and any fixed t $(0 < t < 1)$. The analysis leading to (6) is valid only for $0 \leqslant n \leqslant 2$ [the integral in (6a) being only conditionally convergent for $\lambda \neq 0$ if

$n = 0$]; if $n \geqslant 3$ then $e_2 = 0(h^2)$ since $u(x, t)$ is at least three times differentiable. Note that, if $n \geqslant 4$ then $E_2(\lambda, t)$ is divergent and that (6) is not valid for $t \sim 0$ or $t \sim 1$ when end effects (boundary conditions) are important.

Similarly, the fourth-order scheme

$$\frac{\partial u_4(x, t)}{\partial t} + \frac{8u_4(x + h, t) - 8u_4(x - h, t) - u_4(x + 2h, t) + u_4(x - 2h, t)}{12h} = 0 \quad (7)$$

gives, with periodic boundary conditions, the following approximation to (3):

$$u_4(x, t) = D \sum_{\substack{k=-\infty \\ k \neq 0}}^{\infty} \frac{1}{(2\pi ik)^{n+1}} \exp\{2\pi ik(x - [8 \sin 2\pi kh - \sin 4\pi kh]t/12\pi kh)\}.$$

Consequently, analysis similar to that leading from (5) to (6) gives the asymptotic estimate for the error $e_4(x, t)$:

$$e_4(x, t) \sim E_4(\lambda', t) \qquad (h \to 0), \quad (8a)$$

$$E_4(\lambda', t) = C' \int_{-\infty}^{\infty} \xi^{-n-1} e^{i\lambda'\xi}(e^{i\xi^5} - 1)\, d\xi, \quad (8b)$$

where

$$C' = (D/2\pi)\, i^{-n+1}(h^4 t/30)^{n/5}, \quad (8b)$$

$$\lambda' = (30/h^4 t)^{1/5}(x - t), \quad (8d)$$

provided that $0 \leqslant n \leqslant 4$. If $n \geqslant 5$, the fourth-order scheme (7) gives $e_4(x, t) = 0(h^4)$.

It follows from (6) that, if $x - t = 0(h^{2/3})$, then $e_2(x, t) = 0(h^{2n/3})$ as $h \to 0$ for $0 \leqslant n \leqslant 2$. On the other hand, it follows from (8) that, if $x - t = 0(h^{4/5})$, then the fourth-order scheme gives $e_4(x, t) = 0(h^{4n/5})$ if $0 \leqslant n \leqslant 4$. In general, a centered pth order numerical scheme gives errors $e_p(x, t)$ that behave as

$$e_p(x, t) = \begin{cases} 0(h^{pn/p+1}), & n \leqslant p, \quad x - t = 0(h^{p/p+1}), \\ 0(h^{n+1/2}), & n \leqslant p - 1, \quad x - t = 0(1) < 0, \\ 0(h^p), & \text{otherwise}, \end{cases} \quad (9)$$

where $u(x, t)$ is at least $p + 1$ times differentiable for $x \neq t$ and has a discontinuous nth derivative on $x = t$. Examples of (9) for $x < t$ are given below. Consequently, the L_2 error is $0(h^{p(n+1/2)/p+1})$ if $n \leqslant p$ and $0(h^p)$ if $n \geqslant p + 1$.

In addition to giving the order of magnitude of the error, the results (6) and (8) give the spatial structure of the asymptotic error near $x = t$. We have studied the functions defined by (6) and (8) both by asymptotic analysis and by numerical quadrature for $n = 1$, when the solution has a discontinuous first derivative. Similar analysis applies to other values of n.

Asymptotic analysis by the method of steepest descents (see the Appendix) gives the asymptotic results (for $n = 1$)

$$E_2(\lambda, t) \sim -D\pi^{-1/2}2^{-4/3}3^{5/12}h^{2/3}t^{1/3}\lambda^{-5/4}\exp[-2(\lambda/3)^{3/2}], \qquad (\lambda \to +\infty), \quad (10a)$$

$$E_2(\lambda, t) \sim D\pi^{-1/2}2^{-5/3}3^{5/12}h^{2/3}t^{1/3} \mid \lambda \mid^{-5/4}[\cos(2 \mid \lambda/3 \mid^{3/2}) + \sin(2 \mid \lambda/3 \mid^{3/2})], \qquad (\lambda \to -\infty), \quad (10b)$$

where λ is given by (6c). Similarly, it is found from (8) that (for $n = 1$)

$$E_4(\lambda', t) \sim D\pi^{-1/2}2^{-29/20}3^{-1/5}5^{7/40}(\sqrt{2} - 1)^{-1/2}h^{4/5}t^{1/5}(\lambda')^{-7/8} \cdot \exp[-16(\lambda'/20)^{5/4}]\{\sin[16(\lambda'/20)^{5/4}] - (\sqrt{2} - 1)\cos[16(\lambda'/20)^{5/4}]\}, \qquad (\lambda' \to +\infty), \quad (11a)$$

$$E_4(\lambda', t) \sim D\pi^{-1/2}2^{-6/5}3^{-1/5}5^{7/40}h^{4/5}t^{1/5} \mid \lambda' \mid^{-7/8} \cdot [\cos(4 \mid \lambda'/5 \mid^{5/4}) + \sin(4 \mid \lambda'/5 \mid^{5/4})], \qquad (\lambda' \to -\infty) \quad (11b)$$

where λ' is given by (8d). It follows from these asymptotic results that the error decays exponentially ahead of the discontinuity at $x = t$ but decays only algebraically behind the discontinuity. Notice also the leading error oscillation exhibited in (11a) for the fourth-order scheme, but its absence in (10a) for the second-order scheme. The results (10a), (11a) show that, as $h \to 0$, the error at fixed $x - t > 0$ is zero to order $h^{p/p+1}$; indeed, analysis of (5) and its analog for $p = 4$ shows that the error at $x - t$ behaves as h^p as $h \to 0$. On the other hand, when $x - t < 0$ is fixed, then the amplitudes of E_2 and E_4 are given by (10b) and (11b) as

$$\mid E_2 \mid \sim D\pi^{-1/2}2^{-5/4}3^{3/2}h^{3/2}t^{3/4} \mid x - t \mid^{-5/4},$$
$$\mid E_4 \mid \sim D\pi^{-1/2}2^{-11/8}3^{-3/8}h^{3/2}t^{3/8} \mid x - t \mid^{-7/8},$$

so that if $x - t \sim 1$ then $\mid E_2 \mid \sim 8.555 \mid E_4 \mid$.

The behavior of $E_2(\lambda, t)$ and $E_4(\lambda', t)$ can also be studied near $\lambda = \lambda' = 0$. In fact, it is not difficult to show that both $\partial E_2(\lambda, t)/\partial\lambda$ and $\partial E_4(\lambda', t)/\partial\lambda'$ are discontinuous while both E_2 and E_4 are continuous at $\lambda = \lambda' = 0$. In fact,

$$E_2(\lambda, t) \sim -Dh^{2/3}t^{1/3}2^{-4/3}3^{1/6}[\pi^{-1}\Gamma(2/3) + 3^{-3/2}(\lambda - 3 \mid \lambda \mid)], \qquad (\lambda \to 0), \quad (12)$$

$$E_4(\lambda, t) \sim -Dh^{4/5}t^{1/5}(3)^{-1/5}[\pi^{-1}\sin(2\pi/5)\,\Gamma(4/5) + 10^{-1}(\lambda - 5 \mid \lambda \mid)], \qquad (\lambda \to 0). \quad (13)$$

The results (12) and (13) show that the maximum asymptotic error occurs precisely at $\lambda = \lambda' = 0$, i.e., $x = t$. Note also that $E_2(\lambda, t)$ and $E_4(\lambda', t)$ are infinitely differentiable for λ and λ' nonzero.

Kreiss (private communication, cf. [5]) has suggested an improved fourth-order scheme. The local asymptotic error is given by (8) with C' decreased by a factor $6^{1/5}$. In effect, h can be $6^{1/4} \simeq 1.57$ times larger to achieve the same local error bound; the same improvement holds for smooth solutions [5].

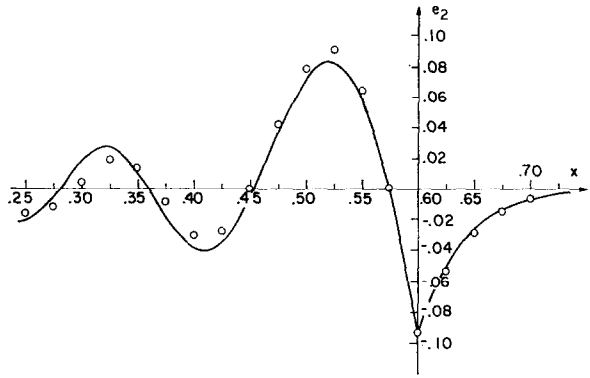

FIG. 1. Comparison of asymptotic and actual local error for second-order scheme (4) for solution of (1) with $f(t) = \sin 2\pi t$ when $h = 1/40$. The results are plotted at $t = .6$. Solid curve: $E_2(\lambda, t)$ plotted as a function of x. Circles: local error at grid points $x = nh$.

In Fig. 1, we plot $E_2(\lambda, t)$ for $h = 1/40$, $t = .6$, $D = 2\pi$ as a function of x. The solid curve is obtained from numerical values of E_2 determined by quadrature (along the steepest descent path to minimize difficulty with the oscillatory integrand of E_2). The data points are the result of numerical integration of the second-order difference scheme (4) with the boundary and initial conditions (1b) and $f(t) = \sin 2\pi t$. This choice of $f(t)$ gives discontinuous first derivatives ($n = 1$). Outflow boundary conditions are applied at $x = 1$ to ensure formal second-order truncation error and the difference equations are integrated with $h = 1/40$ and Adams–Bashforth time differencing with time steps sufficiently small that time differencing errors are negligible. The data points give the pointwise error between the finite-difference and exact solutions to (1) near the discontinuity at $x = t = .6$. Notice the excellent agreement between the theoretical curve for E_2 and the actual error e_2 despite the approximations concerning boundary and initial conditions that entered the theoretical analysis.

A similar comparison between e_4 and E_4 is given in Fig. 2. Here $h = 1/40$, $t = .6$, $f(t) = \sin 2\pi t$. Again, the difference equation (7) is integrated applying (1b) and suitable difference approximations at $x = h, 1 - h, 1$ to ensure the formal fourth-order property of the scheme. The agreement between the theoretical and finite difference results is excellent near the discontinuity.

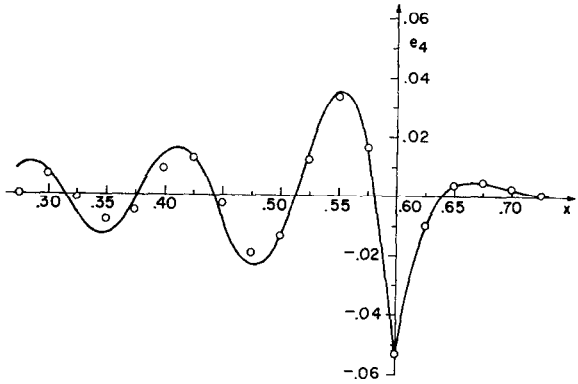

FIG. 2. Same as Fig. 1 only for fourth-order scheme (7). Solid curve: $E_4(\lambda', t)$ plotted as a function of x. Circles local error at grid points $x = nh$.

For comparison, we have also solved the system (1) using a spectral method based on a Galerkin approximation using a Chebyshev polynomial expansion of $u(x, t)$ [5]. This scheme is formally infinite-order accurate, i.e., the error goes to zero faster than any power of $h = 1/N$ as $N \to \infty$, where N is the number of retained Chebyshev polynomials, provided $u(x, t)$ is infinitely differentiable. However, if $u(x, t)$ has a discontinuous nth derivative the error is $0(h^n)$ in the neighborhood of the discontinuity. We have not found a completely satisfactory theory of this local error but numerical experiments confirm that the maximum error when $n = 1$ is roughly $Dh/2\pi$ (cf. [5]). The basis for this estimate is the following argument. When $0 < t < 1$, the discontinuity is located in the interior of the interval $0 < x < 1$. A variation of the argument that led to (5) suggests that the local error is given by

$$e_\infty(x, t) = -D \sum_{|k|>N/\pi} \frac{1}{(2\pi ik)^{n+1}} e^{2\pi ik(x-t)} \tag{14}$$

so that the maximum error occurs at $x = t$ and is given roughly by

$$E_\infty(t, t) \sim Di^{-n-1}\pi^{-1}2^{-n}h^n n^{-1}. \tag{15}$$

The cutoff N/π is used instead of N in (14) because of the special structure of Chebyshev polynomials whereby π polynomials are required per wavelength of smooth solution [5]. The relation (15) is in excellent agreement with numerical experiments [5]. However, this cannot be the whole story since (14) predicts that the error is symmetrical about $x = t$ while calculations show that it is not.

In Fig. 3 we have plotted the actual errors e_2, e_4 and e_∞ for the second-order, fourth-order, and Chebyshev schemes, respectively, with $h = 1/40$, $t = .6$, and the boundary condition $f(t) = \sin 2\pi t$. It is apparent that higher-order schemes

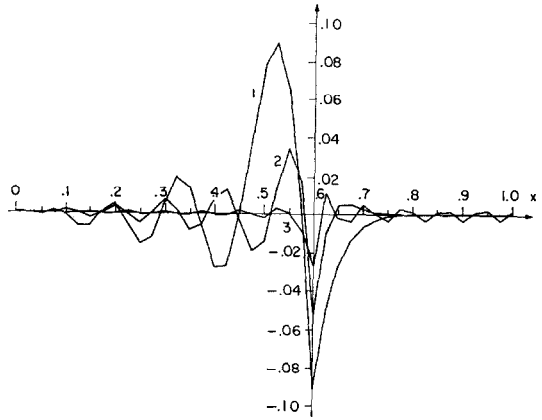

FIG. 3. Local error in numerical solution of (1) with $f(t) = \sin 2\pi t$, $h = 1/40$ at time $t = .6$. Curve 1: second-order scheme [Eq. (4)]. Curve 2: fourth-order scheme [Eq. (7)]. Curve 3: Spectral (Chebyshev) scheme using $N = 1/h$ polynomials [5].

have smaller local errors. In fact, even with roughly 10% local error, as in Fig. 3, Chebyshev (spectral) schemes require at least a factor two less resolution to achieve the same accuracy as fourth-order schemes while fourth-order schemes require a factor two less resolution than second-order schemes, as shown previously [6].

The theory of local errors presented here also explains the 'wakes of bad numbers' observed in test problems of two-dimensional advection of a passive scalar [7]. An example, is given in Fig. 4: the two-dimensional initial conical distribution of scalar $A(x, y)$ shown in perspective in Fig. 4(a) in (x, y, A) space is subjected to uniform rotation about the center of the plotted x, y space. Details of initial conditions are given in Ref. [7]. The result after one full revolution using a 32×32 space grid and a second-order (Arakawa) scheme is shown in Fig. 4(b). If the simulations

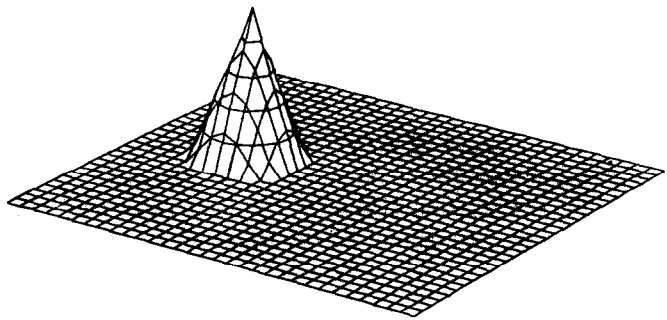

FIG. 4(a). Three-dimensional (x, y, A) perspective plot of initial conditions used in scalar convection test problem.

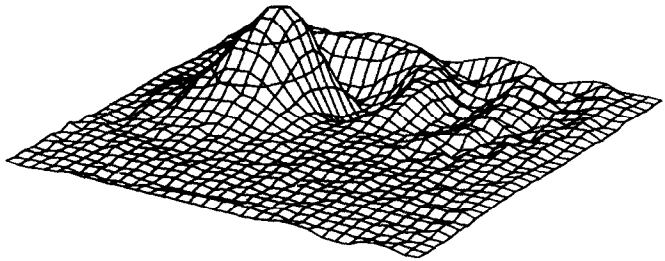

FIG. 4(b). Three-dimensional (x, y, A) perspective plot of the $A(x, y, t)$ field obtained after one revolution using the second-order Arakawa scheme on a 32×32 space grid.

were exact Fig. 4(b) would be identical to Fig. 4(a). According to the theory of the present paper, the large amplitude error waves are mostly due to the discontinuous slopes (sharp corners) of the initial conical distribution.

We have also studied the behavior of local errors when $n \neq 1$. An important case is $n = 0$ where the solution exhibits a jump discontinuity at $x = t$. In this case, it is not difficult to show from (6) that

$$E_2(\lambda) = D \operatorname{sgn} \lambda \int_{|\lambda/3^{1/2}|}^{\infty} Ai(t \operatorname{sgn} \lambda)\, dt \tag{16}$$

where $\operatorname{sgn} \lambda$ is the sign of λ and $Ai(x)$ is the Airy function. Consequently, $E_2(\lambda)$ decays exponentially as $\lambda \to +\infty$, oscillates and decays algebraically as $|\lambda|^{-3/4}$ for $\lambda \to -\infty$, and approaches $+D/3$ as $\lambda \to 0+$ and $-2D/3$ as $\lambda \to 0-$. Similarly, the fourth-order scheme (7) gives $E_4(\lambda)$ that decays exponentially as $\lambda \to +\infty$, algebraically as $|\lambda|^{-5/8}$ for $\lambda \to -\infty$, and approaches $+2D/5$ as $\lambda \to 0+$, and $-3D/5$ as $\lambda \to 0-$.

Finally, we take issue with the often repeated argument that low-order numerical schemes are the most appropriate for the simulation of discontinuous solutions. The present paper shows that, as the order of the schemes increases, the maximum local error and the errors for fixed $x < t$ decrease substantially. Also, as the order of the scheme increases so does the spatial frequency of the spatial error oscillations in the region $x < t$, $x - t = 0(1)$. Consequently, if dissipation is added to smooth the solutions, the required dissipation can be smaller and more localized with high-order schemes, so that dissipative terms have less effect on the solution outside the discontinuous layer.

APPENDIX

In this Appendix, we outline the application of the method of steepest descents to the integral representation (6a) of $E_2(\lambda, t)$ as $\lambda \to -\infty$ in order to establish the asymptotic result (10b). Similar calculations establish (10a) and (11).

Setting $\alpha = (|\lambda|/3)^{1/2}$ and $\xi = \alpha s$, it follows from (6a) that, for $\lambda < 0$,

$$E_2(\lambda, t) = C\alpha^{-n} \int_{-\infty}^{\infty} s^{-n-1} e^{-3i\alpha^3 s} (e^{i\alpha^3 s^3} - 1)\, ds. \tag{A.1}$$

Next the contour of integration (real axis) in (A.1) is deformed into a contour Γ which passes above 0 in the complex s-plane, so that

$$E_2(\lambda, t) = C\alpha^{-n} \left[\int_{\Gamma} s^{-n-1} e^{i\alpha^3(s^3 - 3s)}\, ds - \int_{\Gamma} s^{-n-1} e^{-3i\alpha^3 s}\, ds \right]. \tag{A.2}$$

The second integral in (A.2) is identically zero, as shown by closing the contour Γ in the upper half-plane.

The method of steepest descents is applied to the first integral in (A.2) as follows. The saddle points of the exponential integrand occur where $d(s^3 - 3s)/ds = 0$, i.e., $s = \pm 1$. The contours of steepest descent through the saddle points $s = \pm 1$ are the curves

$$\mathrm{Im}[i\alpha^3(s^3 - 3s)] = \mp 2\alpha^3, \qquad \mathrm{Re}[i\alpha^3(s^3 - 3s)] < 0. \tag{A.3}$$

The curve of steepest descent through the saddle at $s = 1$ is the curve Γ_2

$$v = ((1/3)\, u^2 - 1 + (2/3)\, u^{-1})^{1/2}\, \mathrm{sgn}(u - 1) \qquad (u > 0)$$

where $s = u + iv$. Similarly, the curve of steepest descent through $s = -1$ is Γ_1

$$v = ((1/3)\, u^2 - 1 - (2/3)\, u^{-1})^{1/2}\, \mathrm{sgn}(-u - 1), \qquad (u < 0).$$

Notice that because of (A.3) the exponential integrand of (A.2) goes to zero as $s \to \infty$ along the curves Γ_1 and Γ_2. Consequently, the first contour integral in (A.2) can be deformed into a sum of integrals over Γ_1 and Γ_2. Consider the leading-order behavior of

$$I_1 = \int_{\Gamma_1} s^{-n-1} e^{i\alpha^3(s^3 - 3s)}\, ds$$

as $\alpha \to \infty$. Since $dv/du = -1$ on Γ_1 at $s = -1$, it follows that

$$I_1 \sim \int_{\Gamma_1'} s^{-n-1} e^{i\alpha^3(s^3 - 3s)}\, ds \qquad (\alpha \to \infty)$$

where Γ_1' is the line segment $|u| < \epsilon$, $s = -1 + (1 - i)\, u$ with $\epsilon = \epsilon(\alpha)$ chosen so that $0 < \epsilon(\alpha) < 1$, $\alpha^{3/2}\epsilon(\alpha) \to \infty$ as $\alpha \to \infty$. Consequently,

$$\begin{aligned} I_1 &\sim (-1)^{-n-1}\, (1 - i)\, e^{2i\alpha^3} \int_{-\infty}^{\infty} e^{-6\alpha^3 u^2}\, du \qquad (\alpha \to \infty) \\ &= (-1)^{-n-1}\, \pi^{1/2} 6^{-1/2} \alpha^{-3/2} (1 - i)\, e^{2i\alpha^3}. \end{aligned} \tag{A.4}$$

The integral over Γ_2 necessary to complete evaluation of (A.2) is evaluated similarly. The final result of these calculations is (10b).

REFERENCES

1. G. W. HEDSTROM, *SIAM J. Numer. Anal.* **5** (1968), 363.
2. V. THOMÉE, *SIAM Review* **11** (1969), 152.
3. P. BRENNER AND V. THOMÉE, *Math. Scand.* **28** (1971), 329.
4. H. O. KREISS AND J. OLIGER, "Methods for the Approximate Solution of Time Dependent Problems," GARP Publ. Ser. No. 10, World Meteor. Org.
5. S. A. ORSZAG AND M. ISRAELI, *Ann. Rev. Fluid Mech.* **6** (1974), in press.
6. See references given in [5].
7. S. A. ORSZAG, *J. Fluid Mech.* **49** (1971), 75.

Printed in Belgium